Transient Amplification and Contact Line Instability

Jennifer Rieser

gtg923g@mail.gatech.edu

School of Physics

Georgia Institute of Technology

May 8, 2005

Abstract

Instability in spreading thin liquid films arises from the influence of a driving force and results in the distortion of the leading edge of the film (the contact line). We study this instability in thin films placed on a horizontal substrate and driven by an induced surface tension gradient. We achieve controlled evolution of the contact line distortion by imposing optical perturbations behind the contact line at the onset of the instability. This enables us to directly measure the magnitude of both the initial and evolved disturbances, the ratio of which is defined to be the transient amplification. From a theoretical perspective, the presence of transient amplification is predicted from the non-normality of linearized evolution operator. In this paper, we compare the experimentally measured values of transient amplification to theoretically calculated values. Preliminary results suggest that one may predict transient amplification from the base state of the system provided the size and shape of the imposed disturbance are known.

1 Introduction

Contact line instability in thin films results from the influence of a driving force. An everyday example of this involves painting a wall. When too much paint is applied to a wall, it flows down the wall. Initially, the leading edge (*contact line*) is straight, but as gravity continues to drive the paint down the wall the contact line becomes distorted and drips (fingers) form.

In this example, instability results from small disturbances caused by the texture of the wall. We are interested in studying how such intially small disturbances grow in time. In fact, how much these disturbances have grown is closely related to what we call the *transient amplification*.

Transient amplification is important not only in these studies, but is also related to similar phenomena in other systems (the transition to turbulence). Nevertheless, transient amplification is much easier to study in the context of thin films because their flows do not become turbulent as the Reynolds number is small ($Re << 1$) [1]. Once understood in this simpler context, we hope the knowledge of transient amplification can provide insight into more complicated systems.

2 Theoretical Background

We study the spreading of a thermally driven thin film on a horizontal surface. This flow is governed by conservation laws (momentum, energy, and mass) described by the Navier-Stokes equations. In the case of slowly moving films ($Re << 1$), these equations can be simplified, using the lubrication approximation (which involves depth averaging the fluid velocity over the film thickness), to a single partial differential equation for the film thickness [2]. The behavior of small disturbances is described by the linearized evolution operator of this partial differential equation, the eigenfunctions of which are not orthogonal. That is, the linearized evolution operator is said to be *non-normal*[1]. This can lead to transient amplification.

The concept of non-normality is best understood by a simple example. Consider a two-dimensional system whose time-evolution (at least near the equilibria) is governed by two eigenvalues and their corresponding eigenvectors. In a "normal" system, these eigenvectors are orthogonal, and the dynamics of the system is determined entirely by the time-evolution of the norm of the eigenvectors, whose growth/decay rates are determined by the eigenvalues (Fig. 1a,b). In a non-normal system, however, the eigenvectors are not orthogonal(Fig. 1c,d). As a result, linear stability analysis fails to capture the short-term (transient) behavior of the system. In the case of two negative eigenvalues, the exponential decay predicted by the eigenvalues can be preceded by an initial transient growth, but the system still eventually approaches equilibrium. However, when there is one positive eigenvalue, as is

[1] Mathematically, non-normal means that $LL^\dagger \neq L^\dagger L$, where L is the linearized evolution operator and $L^\dagger$ is its adjoint.

the case for our studies, transient growth has more significant implications. If this transient growth is sufficiently strong, it can push the system far enough away from equilibrium so that it enters a regime in which nonlinear terms can no longer be neglected.

The strength of this growth is related to the transient amplification and, in fact, we formally define transient amplification for these studies to be the amount by which the transient growth of an initially small disturbance has amplified the contact line distortion beyond what is predicted by the positive eigenvalue. It is then natural to consider an *optimal disturbance* or a disturbance that produces the maximum transient amplification for given initial conditions. The structure of such a disturbance is simply a uniform displacement of fluid by some small amount that spans the entire system. This slight increase in fluid results in faster flow[2] and at later times the perturbed fluid is more advanced than the unperturbed fluid. The resulting disturbance amplitude is given by volume conservation.

Numerical computation of the maximum transient amplification resulting from optimal disturbances has been done [2], and these values provide us with an upper bound for what we expect to see experimentally.

3 Experimental Background

To study contact line instability experimentally, we project a light gradient onto a thin film of silicone oil on horizontal substrate (Fig. 2). This light

[2]compared to the unperturbed film as fluid velocity is directly proportional to film thickness

gradient induces a temperature gradient, which then produces a surface tension gradient across the film. This, in turn, drives fluid flow from warmer regions to colder regions (i.e, from regions of higher surface tension to those of lower surface tension) [3]. Once fluid flow has been established, the film reaches an equilibrium shape that depends on the driving force (Fig. 3). Ambient perturbations may then cause instability in the contact line and finger formation. This alone does not provide much insight into how to characterize the transient amplification, as it is difficult to quantify the ambient perturbations and their impact on the system. However, we can quantify the initial disturbance by applying controlled perturbations after the equilibrium has been reached but before the contact line becomes distorted. The contact line instability then evolves in a controlled fashion, so we can characterize quantitatively the effect of applied perturbations and the resulting transient amplification.

In our experiments, we apply sinusoidal optical perturbations, in the form of alternating light and dark bands, to the oil behind the contact line in a direction transverse to the previously established fluid flow (Fig. 4). These perturbations indirectly induce local fluid flow from warmer regions to colder regions, causing local variations in film thickness (Fig. 5) and ultimately resulting in finger formation at the locations of local elevations.

4 Experimental Measurements

Experimentally, transient amplification γ is defined as

$$\gamma \equiv \frac{\|\delta h_f\|}{\|\delta h_i\|} \exp(-\beta t) \tag{1}$$

where $\|\delta h_f\|$ is the magnitude of the final disturbance and $\|\delta h_i\|$ is the magnitude of the initial disturbance. Both of these are characterized by film displacements with respect to the unperturbed film. One also factors out a background exponential growth rate, $\exp(-\beta t)$, that is always present. If growth is purely exponential, then the ratio $\frac{\|\delta h_f\|}{\|\delta h_i\|}$ equals $\exp(\beta t)$, where t is the elapsed time between measurements of δh_i and δh_f. Therefore, transient amplification must always be at least one, with equality holding when growth is purely exponential (equivalently, when the disturbance is not transiently amplified).

For our experiments,

$$\gamma = \frac{f(x = A(t_f))}{h_i(t_i)} \exp(-\beta(t_f - t_i)) \tag{2}$$

The magnitude of the initial disturbance h_i, measured via interferometry, is characterized by the height (depth) of the local elevations (depressions) that result from the applied optical perturbations at time t_i.

One determines the magnitude of the final disturbance by measuring the difference in film thickness between the perturbed and unperturbed film at some horizontal location. For convenience, we choose the location of the unperturbed contact line, at which this difference simplifies to the height of the perturbed film at the unperturbed contact line[3]. We find that the unperturbed contact line location is most easily found if we approximate the fingers as sinusoidal. The location of the unperturbed contact line (for a film driven for the same amount of time as the perturbed film) is then halfway between the maximum and minimum of the sine curve. Therefore,

[3] the film height of the unperturbed film at the unperturbed contact line is always zero by definition of the contact line

the horizontal displacement of the contact line due to the perturbation is equal to the amplitude of the sine wave. The height of the perturbed film at the unperturbed contact line is then found by evaluating a polynomial fit $f(x)$ of the film profile with horizontal position x equal to the amplitude A of the fingers at time t_f (Fig. 6). We determine the exponential growth rate by plotting the natural log of the finger amplitude as a function of time and estimating the slope of the linear region (Fig. 7).

5 Theoretical Calculations

To solve the partial differential equation for film thickenss (described earlier), boundary conditions need to be specified. In the slip model [2], these boundary conditions are specified by a slip coefficient (which allows for a difference in velocity between the fluid and the substrate) and the microscopic slope of the fluid at the contact line. As these values cannot be extracted from experimental data, they are used as free parameters to fit the model to the experimentally determined film profile of the undisturbed flow (8). Using this as the base state, the evolution of small disturbances to this state is computed numerically.

As mentioned earlier, an optimal disturbance is defined to be a uniform displacement of fluid that spans the entire system. Calculating the resulting transient amplification provides an upper bound for experimentally observed disturbances, as actual disturbances are sub-optimal in that they neither span the entire film nor displace the fluid uniformly. Although this provides us with an upper limit, we find the behavior of the resulting transient amplification from experimental and optimal disturbances to be too different to make quantitative comparisons. Accordingly, we are studying experimentally realistic disturbances numerically.

6 Results

In order to compute numerically the transient amplification for sub-optimal disturbances, we also need to extract the disturbance profile from the experimental data and input it into the model along with the fitted base state. Upon reviewing our preliminary results (Fig. 9), we realized that our calculations need to be revised. First, both our experimental measurements and theoretical computations yield transient amplification are less than unity. We consider these seemingly contradictory results for experimental measurements and numerical computations separately.

The numerical model used in these calculations was initially constructed to calculate transient amplification resulting from optimal disturbances. Recall that optimal disturbances span the entire system and are therefore immediately at the contact line. In this case, the computation of transient amplification beginning at $t = 0$ makes sense, as the disturbance is instantaneously at the contact line. However, for non-optimal disturbances located away from the contact line, we expect to observe some propagation time that must elapse before the imposed disturbance actually reaches the contact line. Consequently it does not make sense to factor out the exponential growth rate of the disturbance at the contact line when the disturbance is not yet there. At present, we are modifying the model to determine this propagation time and to begin computating the transient amplification at this time.

Experimentally, the time-evolution of the transient amplification can be explained by two effects. The first of these is identical to the modification required for the numerical model. The imposed disturbance is not instantaneously located at the contact line; instead, there is some propagation time present that must be incorporated. Second, the contact line distortion as a function of time exhibits rather peculiar behavior (Fig. 10). The contact line distortion grows initially, then disappears entirely, and finally reappears later. This unexpected behavior is actually the result of a secondary thermal effect of the perturbation. While the perturbation is applied, a temperature gradient develops in the fluid between the contact line and the location of the applied perturbations. As a result, the fluid in the vicinity of the light bands of the perturbation advances faster than that in the dark regions (this corresponds to the first peak in fig. 10). Once the perturbation is turned off, this effect immediately begins to vanish, and regions corresponding to dark bands move faster. In fact, this fluid reaches and then advances beyond the fluid that was pushed ahead by the light perturbations. We are presently correcting our measurements to account for this.

7 Conclusions

There have been claims that non-normality explains the transition to turbulence in many fluid flow problems [4], however, no quantitative comparisons between experiment and theory currently exist.

Modifications we made to the existing experimental model allow us for the first time to calculate transient amplification for sub-optimal disturbances by inputting the experimentally determined disturbance profile into the computational model. We find that transient amplification values for sub-optimal disturbances that are located away from the contact line have an associated time delay as there is some amount of time required for these disturbances to propagate to the contact line.

Preliminary results suggest that quantitative comparisons between experiment and theory as well as possibly even theoretical predictions of transient amplification for given initial conditions are possible.

Acknowledgements

I would like to thank Dr. Michael Schatz and Dr. Roman Grigoriev for their ongoing guidance, commitment, advice, and support throughout this project. I would also like to thank Mason Porter and Slaven Peles for serving as advisors. Others who offered their support and deserve thanks include Kyoko Kamei for her patience and my initial training, Kapil Krishan and Vivek Sharma for numerous helpful discussions, and Ed Greco for his assistance with Matlab.

References

[1] D. J. Tritton. *Physical Fluid Dynamics.* Oxford University Press, New York, second edition, 1988.

[2] R. O. Grigoriev. Contact line instability and pattern selection in thermally driven liquid films. *Phys. Fluids*, 15:1363–1374, 2003.

[3] Nicholas Garnier, Roman O. Grigoriev, and Michael F. Schatz. Optical manipulation of microscale fluid flow. *Phys. Rev. Lett.*, 5:054501–1–054501–4, 2003.

[4] Lloyd N. Trefethen, Anne. E. Trefethen, Satish C. Reddy, and Tobin A. Driscoll. Generalized stability theory part i: Autonomous operators. *J. Atmos. Sci.*, 53:2025, 1996.

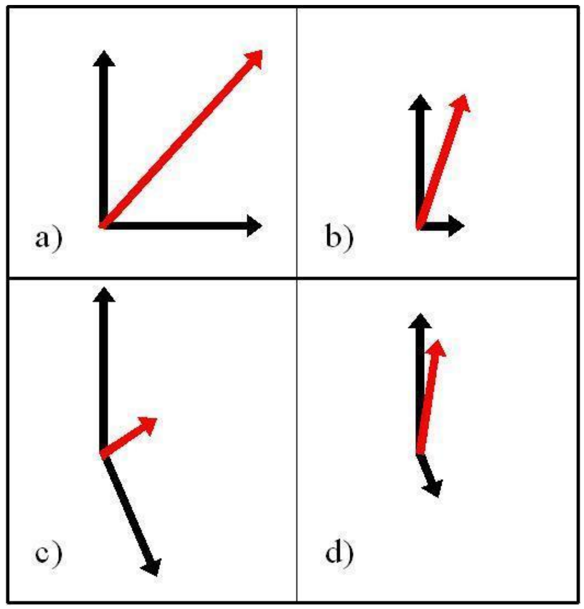

Figure 1: (a) Two orthogonal eigenvectors (black) and their resulting norm (red). (b) Time evolved eigenvectors (black) and their norm (red) for the case of two negative eigenvalues. The magnitudes of both vectors will decay monotonically in time, and it is therefore expected (from standard linear stability analysis) that their norm will behave in a similar manner. In fact, this is indeed the case when the vectors are orthogonal. However, the situation is much different when eigenvectors are not orthogonal, as in (c) and (d). (d) represents the time-evolution of vectors in (c), both of which have negative eigenvalues. Despite the fact that the magnitudes of both eigenvectors decrease, the norm of the two actually experiences a transient growth that precedes the decay predicted by standard linear stability analysis.

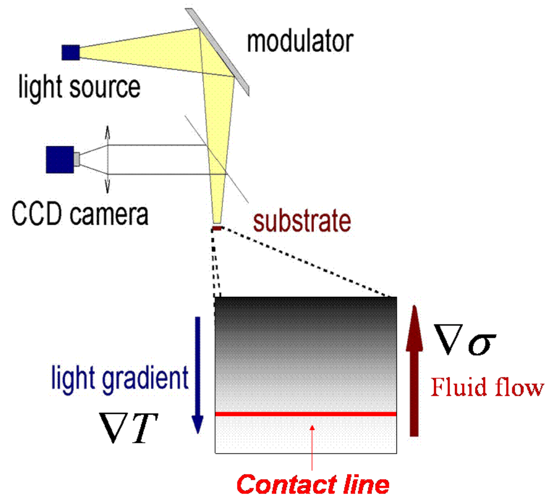

Figure 2: Initial experimental setup. Light is projected onto the substrate on which the oil has been placed. (The substrate has been enlarged and rotated in the lower portion of the figure.) The oil placed on the substrate is below the contact line (shown in red). The applied light gradient indirectly induces a surface tension gradient, driving fluid flow toward the darker region.

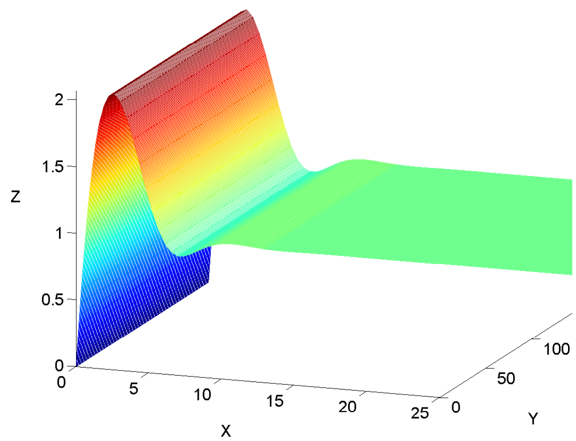

Figure 3: Theoretically predicted base (initial) state of film. Experimentally, this state is achieved by an induced surface tension gradient. Color represents film height, ranging from 0 (blue) to 2 (red) in non-dimensional units. Fluid flows toward the negative x direction, the y direction is transverse to the fluid flow, and the vertical axis gives the film thickness in non-dimensional units.

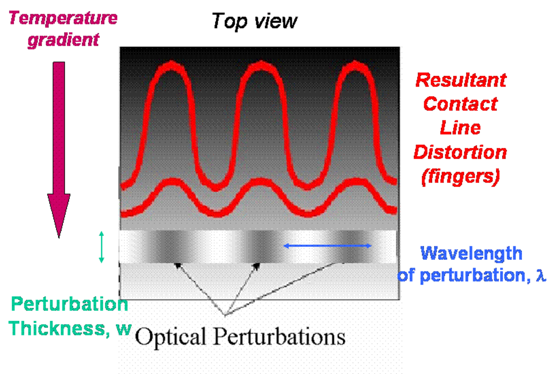

Figure 4: Depiction of applied optical perturbations and resulting fingers. Perturbations are applied while the contact line is still straight, and fingers form after the perturbations are turned off. We vary both the wavelength and width of the perturbations effectively controlling the size of the resulting disturbance.

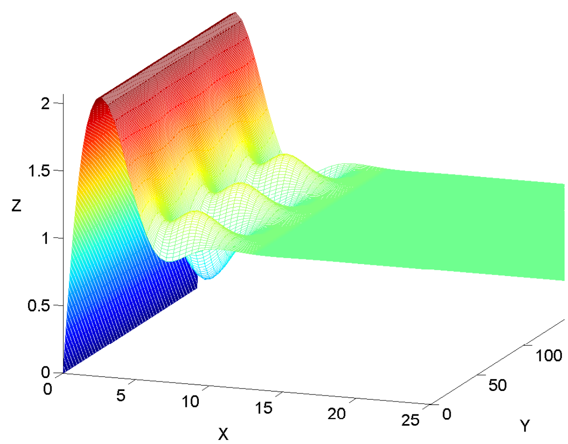

Figure 5: Film just after perturbations have been applied. The local variations in film thickness behind the contact line are a result of the applied perturbations. Color represents film height, ranging from 0 (blue) to 2 (red) in non-dimensional units. Fluid flows toward the negative x direction, the y direction is transverse to the fluid flow, and the vertical axis gives the film thickness in non-dimensional units.

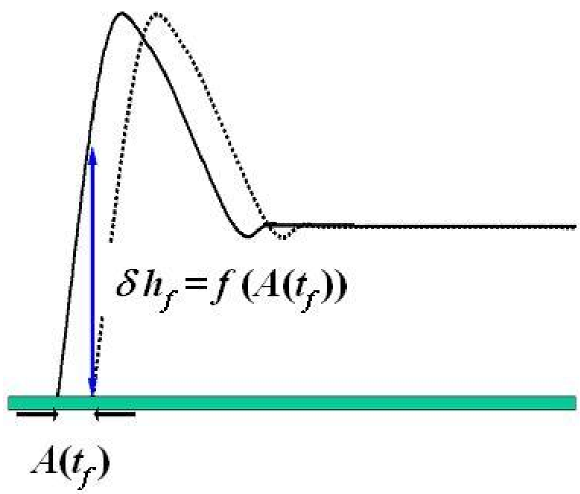

Figure 6: Measurement of the magnitude of final disturbance δh_f. The dotted line represents the unperturbed profile, and the solid line represents the perturbed profile. The magnitude of the final disturbance is measured at the location of the unperturbed contact line by evaluating a polynomial fit $f(x)$ of the perturbed profile height at the finger amplitude $x = A$. That is, we determine the horizontal distance between the perturbed and unperturbed contact lines. This finger amplitude grows with time and is evaluated at t_f.

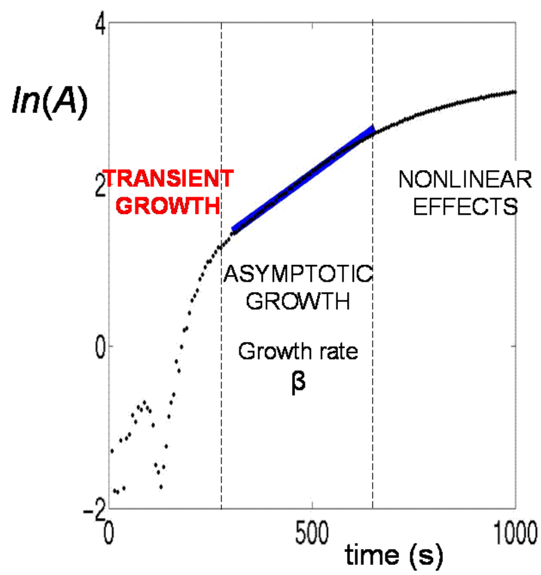

Figure 7: Natural log of finger amplitude as a function of time. The first region shows transient growth, the middle region shows exponential growth, and the right region represents when nonlinear terms become significant.

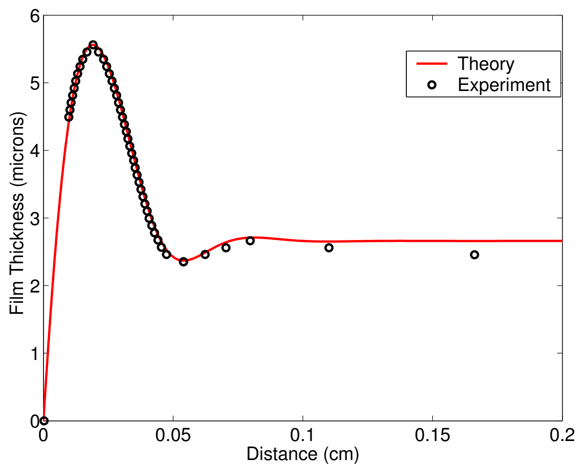

Figure 8: Theoretical fit of initial experimental film profile (prior to onset of instability) achieved by optimizing two free parameters. The differences in the tail thickness result from the fact that theoretical calculations consider a constant fluid flux at the tail while the total volume of fluid is constant in experiments.

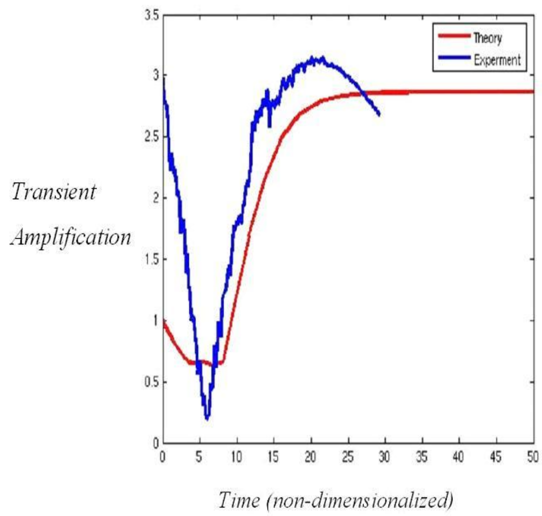

Figure 9: Numerically calculated and experimentally measured transient amplification as a function of time. The dip in transient amplification below one in the theory (red) is attributed to a time delay related to the propagation time required for a disturbance to reach the contact line. Experimentally, the dip in transient amplification results in part from the propagation time of the disturbance and in part from a secondary thermal effect that results from applied perturbations.

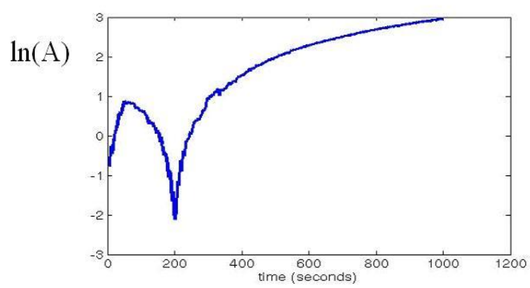

Figure 10: Contact line distortion (natural log of the finger amplitude) as a function of time (seconds). The initial peak is a consequence of a secondary thermal effect that results from the applied perturbations. Once the thermal disturbances dissipate (dip at $t = 200$), the contact line experiences the expected distortion.